Published in final edited form as:

J Am Soc Mass Spectrom. 2021 February 03; 32(2): 455–464. doi:10.1021/jasms.0c00348.

Localization of carbon-carbon double bond and cyclopropane sites in cardiolipins via gas-phase charge inversion reactions

Caitlin E. Randolph[†], **De'Shovon M. Shenault**[†], **Stephen J. Blanksby**[‡], **Scott A. McLuckey**[†,*]

[†]Department of Chemistry, Purdue University, West Lafayette, Indiana 47907-2084, USA

[‡]Central Analytical Research Facility, Institute for Future Environments, Queensland University of Technology, Brisbane, QLD 4000, Australia

Abstract

Cardiolipins (CLs) are comprised of two phosphatic acid moieties bound to a central glycerol backbone and are substituted with four acyl chains. Consequently, a vast number of distinct CL structures are possible in different biological contexts, representing a significant analytical challenge. Electrospray ionization tandem mass spectrometry (ESI-MS/MS) has become a widely used approach for the detection, characterization, and quantitation of complex lipids, including CLs. Central to this approach is fragmentation of the $[CLs - H]^-$ or $[CL - 2H]^{2-}$ anions by collision-induced dissociation (CID). Product ions in the resulting tandem mass spectra confirm the CL subclass assignment and reveal the numbers of carbons and degrees of unsaturation in each of the acyl chains. Conventional CID, however, affords limited structural elucidation of the fatty acyl chains, failing to discriminate isomers arising from different site(s) of unsaturation or cyclopropanation and potentially obscuring their metabolic origins. Here, we report the application of charge inversion ion/ion chemistry in the gas phase to enhance the structural elucidation of CLs. Briefly, CID of $[CL - H]^{2-}$ anions generated via negative ion ESI allowed for the assignment of individual fatty acyl substituents and phosphatidic acid moieties. Next, gas-phase derivatization of the resulting CL product ions, including fatty acyl carboxylate anions, was effected with gas-phase ion/ion charge inversion reactions with tris-phenanthroline magnesium reagent dications. Subsequent isolation and activation of the charge-inverted fatty acyl complex cations permitted the localization of both carbon-carbon double bond and cyclopropane motifs within each of the four acyl chains of CLs. This approach was applied to the *de novo* elucidation of unknown CLs in a biological extract revealing distinct isomeric populations and regiochemical relationships between double bonds and carbocyles.

Graphical Abstract

[*]Address reprint requests to: Dr. Scott A. McLuckey, 560 Oval Drive, Department of Chemistry, Purdue University, West Lafayette, IN 47907-2084, USA, Phone: (765) 494-5270, Fax: (765) 494-0239, mcluckey@purdue.edu.

Supporting Information. Scheme S1 provides a proposed dissociation mechanism for a cyclopropane containing deprotonated fatty acid bound to $MgPhen^{2+}$.

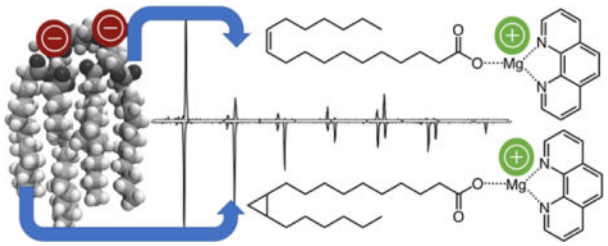

Introduction

Mass spectrometry (MS) is among the most widely adopted techniques in the field of lipidomics.[1, 2] Two prominent MS-based strategies have emerged for routine lipid detection, identification, and quantification. In the first approach, crude lipid extract is separated via some form of chromatography prior to ionization and admission into a mass spectrometer. Recently, the so-called shotgun approach, in which lipid extracts are directly introduced into the mass spectrometer, usually via electrospray ionization (ESI), has gained popularity.[3–5] The measurement of mass (i.e., *m/z* ratios) with high accuracy alone can provide lipid sum composition. By utilizing low-energy collision induced dissociation (CID), partial lipid structural elucidation can be achieved. For acidic glycerophospholipids (GPLs), abundant $[M - H]^-$ precursor ions formed via ESI, fragment to yield product ions permitting the assignment of lipid class and fatty acyl sum composition. However, isomeric GPLs such as sn-positional isomers (i.e., species with different esterification sites along the glycerol backbone) or those arising from differences in structural features like the location and geometry of carbon-carbon double bonds cannot be resolved when relying on low-energy CID alone.[6–8] In turn, as critical structural details remain indistinguishable with conventional MS-based approaches, there is a need for the development of novel tandem MS (MS/MS) workflows for more comprehensive identification and quantitation of lipids in biological samples.

Cardiolipins (CLs) are a unique subclass of GPLs localized virtually completely in the inner mitochondrial membrane where they are required for proper mitochondrial function.[9] Exhibiting distinct chemical and physical properties, CLs are known to play roles in mitochondrial pathways such as electron transport, ATP synthesis, and apoptosis, namely by providing functional and structural stabilization to mitochondrial enzymes.[10–12] Given the fact that CLs are vital to the function of mitochondria, alterations in both CL content and composition can lead to mitochondrial dysfunction. For example, numerous pathologies including Barth syndrome, heart failure, diabetes, and several types of cancer, have been linked to CL deficiencies and acyl chain remodeling.[10, 13–19] A high number of CL structures can be derived from permutations of the four acyl chains,[20] which makes the analysis of acyl chain remodeling a particularly challenging task.

Due to the presence of two acidic phosphatidyl groups, abundant deprotonated CL molecules are generated upon negative ESI.[1] CID of the CL anion, arising from either single or double deprotonation, has been partially successful in characterizing CL structures. Specifically, the MS^2 spectra of deprotonated CL anions facilitates the assignment of phosphatidic acid (PA) moieties and fatty acyl subsitutents.[21] Further fragmentation of

individual $[PA - H]^-$ product ions derived from CL anions in MS^3 experiments allow for identification of fatty acyl composition and regiochemistry. We note, however, that assignments of regiochemistry based on the relative abundances of MS^3 product ions should be made with caution, as products from minor *sn*-positional isomers cannot be excluded.[22] Thus, if possible, authentic CL standards should be used for corroboration of regiochemical assignments. Hsu and Turk reported that the CID spectra of $[CL - 2H + Na]^-$ anion can also be used to reveal fatty acyl and PA composition and tentative regiochemical assignments.[23, 24] We have recently presented an alternative strategy for enhancing the $[CL - H]^-$ ion population (and thus sensitivity) in direct infusion analysis through charge reduction of $[CL - 2H]^{2-}$ dianions via ion/ion reactions.[25] Neither approach can yield insight into the structure and regiochemistry within the acyl chains carried by CLs.

Noting that tandem mass spectrometry methods using low-energy CID cannot distinguish subtle structural features, approaches like those described above fail to discern lipid isomers such as those varying in the site(s) of unsaturation site and geometry. Although a number of novel mass spectrometric approaches have been developed to identify double bond locations in unsaturated lipids,[6, 7] few of these approaches have been applied to CL analysis. Furthermore, while alternative methods such as the Paternò Büchi reaction[26–29] and ozone-induced dissociation (OzID)[30–37] have attracted widespread attention for their abilities to assign the site(s) of unsaturation in the acyl chain substituents of complex lipids, these approaches cannot be extended to localize cyclopropyl moieties. In a notable recent report, Brodbelt et al. implemented 193 nm ultraviolet photodissociation (UVPD) in conjunction with CID to locate carbon-carbon double bonds and cyclopropane rings in CLs derived from a biological extract.[38, 39] The hybrid CID and UVPD method has demonstrated the highest level of structural identification for CL as of this writing. We note, however, that the limited fragmentation efficiency of UVPD for ionized lipids can hinder sensitivity.

Recently, gas-phase ion/ion reaction strategies for the detailed structure elucidation of complex lipids in biological mixtures have been demonstrated.[40–46] In this study, we apply charge inversion ion/ion reactions to facilitate the localization of unsaturation sites in CLs. The approach provides the on-demand ability to switch between charge states after ionization. In particular, utilizing CID of $[CL - 2H]^{2-}$ precursor anions, individual PA and fatty acyl composition can be assigned, while charge inversion of the resulting $[FA - H]^-$ product ions via reaction with dications (*i.e.,* $[MgPhen_3]^{2+}$) permits the unambiguous identification of cyclopropane and unsaturated FAs. Importantly, CID of the $[FA - H + MgPhen]^+$ complex cations originating from cyclopropane FAs yields diagnostic spectra that are fundamentally distinct from their isomeric acyclic counterparts, and therefore, both carbon-carbon double bond and cyclopropane ring unsaturation sites can be confidently pinpointed based upon the product ion spectra of $[FA - H + MgPhen]^+$ ions. Application of the methodology described herein to a CL extract from *Escherichia coli* (*E. coli*) reveals the presence of isomeric CLs that would otherwise be unrecognized by conventional ESI-MS/MS analysis.

Experimental

Materials.

HPLC-grade methanol was obtained from Fisher Scientific (Pittsburgh, Pennsylvania). Magnesium chloride and 1,10-Phenanthroline (Phen) were sourced from MilliporeSigma (St. Louis, MO). The CL standards and *E. coli* CL extract were purchased from Avanti Polar Lipids, Inc. (Alabaster, AL) and used without further purification. FA standards were obtained from Cayman Chemical (Ann Arbor, MI). Solutions of lipid standards (1 μM) were prepared in methanol. To prepare tris-phenanthroline magnesium complexes, the metal salt and 1,10-phenantrholine were mixed 1:1 (mol/mol) in methanol (20 μM). Solutions of *E. coli.* CL extract were prepared in methanol to a final concentration of 50 μM, assuming an average lipid molar mass of 1430 g/mol.

Mass Spectrometry.

Experiments were conducted on a Sciex QTRAP 4000 triple quadrupole/linear ion trap mass spectrometer (SCIEX, Concord, ON, Canada) modified to perform ion/ion reactions.[47] Alternately pulsed nESI permits the sequential injection of lipid anions and tris-phenanthroline magnesium dications.[48] Lipid anions generated by negative nESI were mass-selected by Q1 and transferred to the high-pressure collision cell, q2, for storage. In q2, FA anions are liberated from doubly deprotonated CLs (*i.e.,* $[CL - 2H]^{2-}$) via single frequency resonance excitation (i.e., ion trap CID, q = 0.2). Next, positive nESI produced tris-phenanthroline magnesium dications, denoted $[MgPhen_3]^{2+}$, were isolated by Q1 and stored in the reaction cell q2. The dications and lipid anions were simultaneously stored in q2 for 500 ms. For MS^n experiments in Q3, product cations were isolated (unit resolution) and subjected to ion-trap CID (q = 0.383). In all cases, mass analysis was performed using mass-selective axial ejection (MSAE).[49]

Nomenclature.

The lipid nomenclature described by Liebisch *et. al.*[50] is used here, wherever possible. For example, the fatty acyl class and cardiolipin subclass are abbreviated as FA and CL, respectively. To describe FA structure, we utilize the *X*:*Y* shorthand notation where *X* indicates the total number of carbon atoms and *Y* refers to the degree of unsaturation. Double bond position relative to the carboxylate group is denoted within parenthesis following the colon by a number when the geometry is unknown or, when known, a number followed by geometry (*Z* for cis, *E* for trans). To distinguish between carbon-carbon double bond and cyclopropane motifs we adapt nomenclature proposed by Blevins *et al.*[38] wherein the letter “c” is used to indicate the presence of a “cyclopropane” and the number assigns the position relative to the carboxylate moiety.

To describe CL structure, each fatty acyl substituent is listed sequentially using literature conventions for fatty acyl chain shorthand notations, as described above. Fatty acyl substituents are separated by a forward slash in the case that regiochemical assignments are known. Otherwise, fatty acyl constituents are separated by an underscore. Moreover, we utilize modifications to CL shorthand notation proposed by Macias *et al.*[39] to describe CL structures in which the fatty acyl composition for each PA moiety is known, yet

regiochemical assignments cannot be made. For example, in the case that individual fatty acyl and PA moiety regiochemical assignments cannot be made but the fatty acyl composition of individual PA moieties can be discerned, known PA fatty acyl compositions are indicated within parentheses and an underscore is used to separate individual PA constituents (*e.g.,* CL (16:0_17:1)_(18:0_20:1 indicates a CL comprised of PA 16:0_17:1 and PA 18:0_20:1).

Results and Discussion

Identification of cyclopropane FAs using charge inversion reactions

Recently, we reported the charge inversion of FA anions via gas-phase ion/ion reaction with tris-phenanthroline magnesium dications (*i.e.,* $[MgPhen_3]^{2+}$) to identify carbon-carbon double bond position(s) in unsaturated lipids.[42–44, 46] Briefly, CID of the $[FA - H + MgPhen]^+$ complex cation generates isomer-specific fragmentation patterns that permit unambiguous FA identification via direct spectral interpretation or automated spectral matching to an established CID mass spectral library comprised of charge-inverted FA complex cation CID spectra. Here, we examined the utility of charge inversion chemistry to pinpoint cyclopropane rings within cyclopropane FAs. Scheme 1 details the charge inversion process. Owing to the carboxylic acid moiety, direct negative nESI of phytomonic acid, abbreviated as FA 19:1(c11), yields abundant $[19:1(c11) - H]^-$anions. In an identical fashion as previously described for FAs, ion/ion reactions of $[19:1(c11) - H]^-$anions with $[MgPhen_3]^{2+}$ reagent dications charge invert cyclopropane FAs to the positive ion mode. The product ion spectrum shown in Figure 1a details the results of the ion/ion reaction. Explicitly, the $[19:1(c11) - H + MgPhen_2]^+$ (*m/z* 679.3) cation is the dominant charge-inverted product ion observed (Figure 1a). Energetic transfer of the charge-inverted product ions from the reaction cell q2 to the LIT, referred to as beam-type (BT) CID, generates the CID spectrum presented in Figure 1b. BT CID primarily results in the loss of a single neutral phenanthroline ligand, giving rise to the $[19:1(c11) - H + MgPhen]^+$ (*m/z* 499.2) complex cation (Figure 1b).

The ion-trap CID spectrum of the *m/z* 499.2 ion is shown in Figure 2a. Collisional activation of the charge-inverted FA 19:1(c11) complex cation promoted charge remote fragmentation of the aliphatic chain, as consecutive carbon-carbon single bond (C–C) cleavage generates the series of even-electron (odd-mass) product ions depicted in Figure 2a. By nature of the charge remote fragmentation (CRF) mechanism, the observed structurally diagnostic carboxylate product ions are terminally unsaturated, unless otherwise noted, beginning with C3–C4 fragmentation (*m/z* 275.1) and continuing along the chain. We note that the only odd-electron (even-mass) product ion originating from the aliphatic chain resulted from homolytic C2–C3 cleavage (*m/z* 262.1) and is likely a special case arising from radical stabilization by the adjacent carboxylate moiety. To localize the cyclopropane, diagnostic product ions generated via dual cross-ring carbon-carbon cleavages on both sides of the cyclopropane ring were observed. Explicitly, fragmentation of the cyclopropane ring yields a series of doublet product ions consisting of a dominant CRF ion and a CRF ion with an additional degree of unsaturation, suggested to arise via hydride migrations and CRF, as indicated by the product ions at *m/z* 385.1/387.1 and 399.1/401.1 (Figure

2a). To rationalize the appearance of these product ions, we thus propose that CRF across the cyclopropane rings leads to a ring opening with the subsequent loss of dihydrogen, which allows secondary CRF fragmentation and accounts account for the presence of the doublet product ions corresponding to cyclopropane cross-ring cleavages. The proposed fragmentation mechanism is illustrated in Supporting Information Scheme S1 and could also account for the losses of 98, 84, and 70 Da neutral species. The CID spectrum of [19:1(c11) – H + MgPhen]$^+$ (*m/z* 499.1) contains additional product ion doublets (*m/z* 413.1/415.1 and 427.1/429.1) arising from carbon-carbon bond fragmentation directly following the cyclopropane ring. Lastly, as fragmentation nears the methyl group of the aliphatic chain, a low abundance ion was detected at *m/z* 443.1, representing the heaviest product ion (highest *m/z*) observed upon activation of the charge-inverted FA 19:1(c11) ion.

Importantly, the observed spectral pattern generated via CID of the [19:1(c11) – H + MgPhen]$^+$ product ion is unique to cyclopropane FAs. As such, it should be possible to use these patterns to differentiate cyclopropane FAs from acyclic isomers such as mono-unsaturated FAs (Figure 2). We note that isomeric monounsaturated and cyclopropane FA standards are not commercially available, and thus, direct comparison of the CID spectra of [FA – H + MgPhen]$^+$ complex cations derived from isomeric cyclopropane and monounsaturated FAs cannot be attained. Therefore, we examined FA 19:1(c11) and FA 18:1(11*Z*) using the described ion/ion approach to test the feasibility of charge inversion reactions for the differentiation of unsaturated FAs containing cyclopropane modifications and double bonds. While not isomers, the functionalization in each reference standard is located at the *n*-7 position relative to the methyl group of the aliphatic chain. As evidenced by Figure 2, the CID spectra of the charge-inverted 19:1(c11) and 18:1(11*Z*) complex cations display distinct spectral patterns, leading to product ions and neutral losses indicative of the carbocycle and the double bond, respectively. Consistent with previous observations, interrogation of [18:1(11*Z*) – H + MgPhen]$^+$ gives rise to a spectral gap that indicates double bond location (Figure 2b). Flanking the spectral gap are product ions at *m/z* 359.1 and 413.1/415.1, generated via C–C cleavages allylic to the double bond. The spectral gap highlighted in Figure 2b arises from the suppression of product ions representing cleavages of the C11=C12 double bond (*m/z* 385.1) and C–C fragmentation vinylic to the double bond (*m/z* 373.1 and 399.1). Ultimately, direct spectral interpretation, exploiting the characteristic spectral gap, or automated spectral matching to an established FA library permits C=C localization.[42] However, as many cyclopropane FA standards are not commercially available, CID spectral comparison to an authentic reference standard is not always possible. Notably, the distinct fragmentation pattern as well as neutral losses reveal the presence and location of the cyclopropane ring. In particular, the CID spectrum of [19:1(c11) – H + MgPhen]$^+$ shows neutral losses of 98, 84, and 56 Da, corresponding to the product ions observed at *m/z* 401.1, 415.1, and 443.1, respectively (Figure 2a and c). Significantly, the same neutral losses were not produced, or observed at exceedingly low relative abundances (i.e., <0.5% relative abundance), upon CID of the [18:1(11*Z*) – H + MgPhen]$^+$ cation (Figure 2b and c). To highlight the differences between the two product ion spectra shown in Figure 2a and b, Figure 2c represents the inset data as neutral loss spectra. In turn, together with the distinct fragmentation pattern, these key neutral losses can be exploited to assign both the presence and location of the cyclopropyl moiety. The

expected neutral losses for $[FA - H + MgPhen]^+$ product ions from FAs containing a cyclopropane moiety are listed in Table 1. Though not yet fully understood by ourselves or others, we note that there is likely a difference in the dissociation mechanism(s) between the unsaturated and cyclopropanated chains. That said, the resulting CID spectra in Figure 2 are sufficiently different, and in turn, the direct comparison to the previously generated library spectra will easily distinguish FA structures containing double bonds from those possessing a cyclopropane ring. Even when authentic standards are not available, the comparison of "neutral loss spectra", as highlighted in Figure 2, will provide a robust means to identify the FA functional group.

Identification of CLs using charge inversion reactions

It has been well established that dissociation of $[CL - 2H]^{2-}$ anions generates information related to fatty acyl chain and PA composition. However, the CID spectrum of a doubly deprotonated CL anion fails to define the location(s) of unsaturation. We recently described a top-down shotgun lipidomics approach to achieve near-complete structural determination of glycerophospholipids utilizing gas-phase ion/ion charge inversion and derivatization chemistries.[42, 43] Herein, we extend this approach to characterize the key elements in CL structures, pinpointing acyl chain double bond as well as cyclopropane positions.

To do this experiment, synthetic CL 16:0/18:1(9*Z*)/16:0/18:1(9*Z*) was subjected to negative ion nESI, resulting in abundant $[CL - 2H]^{2-}$ anions detected at *m/z* 701.5. Subsequent ion CID of the mass-selected CL 16:0/18:1(9*Z*)/16:0/18:1(9*Z*) dianion in q2 yields the product ion spectrum shown in Figure 3a. Activation of the $[CL - 2H]^{2-}$ precursor anion promoted formation of abundant $[18:1 - H]^-$ (*m/z* 281.2) and $[16:0 - H]^-$ (*m/z* 255.2) carboxylate anions. Acyl chain composition was also revealed by losses of the 16:0 and 18:1 chains as fatty acids and ketenes as neutral species. In particular, the triacylated CL anions observed at *m/z* 1147.7 and 1121.7 are indicative of 16:0 and 18:1 fatty acid loss, respectively. In addition, the doubly deprotonated product ion at *m/z* 569.4 was formed via neutral loss of the 18:1 acyl chain as a ketene, and similarly, ketene loss of the 16:0 acyl chain resulted in formation of the product dianion at *m/z* 582.4. As evidenced by the product ions at *m/z* 883.6 and 857.5, combined losses of the 16:0 and 18:1 constituents from the doubly deprotonated CL 16:0/18:1(9Z)/16:0/18:1(9Z) ion also serve as diagnostic fragments for CL composition. Confirming individual PA moiety assignment, cleavage of the central glycerol backbone gave rise to the $[PA\ 16:0/18:1 - H + 56]^-$ product ion (*m/z* 729.5), consistent with previous observations by Hsu and Turk.[21] Also indicative of PA composition are the $[PA\ 16:0/18:1 - H - 18:1]^-$ (*m/z* 391.2) and $[PA\ 16:0/18:1 - H - 16:0]^-$ (*m/z* 417.2) ions. Consistent with a previous report[21], we note that liberation of fatty acyl anions from the *sn*-2 (or *sn*-2') position is favored over that of the *sn*-1 (or *sn*-1') linkage in PA precursor ions. For instance, the $[18:1 - H]^-$ (*m/z* 281.2) product ion was observed at a greater abundance than the 16:0 carboxylate anion (*m/z* 255.2). Similar trends were also observed for the singly charged triacylated product ion pair observed at *m/z* 1147.7 and 1121.7 (i.e., 16:0 and 18:1 fatty acid loss respectively) and the analogous doubly deprotonated product ion pairs at *m/z* 569.4 and 582.4 (i.e., neutral loss of the 18:1 and 16:0 acyl chains as a ketenes respectively). Note that for unknown lipids, the relative abundances of the carboxylate anions alone (or related triacylated product ions) are insufficient to assign fatty acyl regiochemistry (*i.e., sn*-1

or *sn*-2) without reference to authentic standards.[22] They can, however, serve as a useful guide as to the most abundant regioisomer.

The charge inversion approach begins with the reaction of CL product anions depicted in Figure 3a with $[MgPhen_3]^{2+}$ dications. The resulting product ion spectrum is portrayed in Figure 3b. Abundant $[16:0 – H + MgPhen_2]^+$ (*m/z* 639.3) and $[18:1 – H + MgPhen_2]^+$ (*m/z* 665.3) complex cations were generated from the ion/ion reaction, along with minor product ions at *m/z* 1505.9 and 1531.9 reflecting the parallel charge-inversion of alternative CID product anions at *m/z* 1121 and 1147.7 (Figure 3b). Subsequent BT CID primarily results in the loss of a single phenanthroline ligand, leading to the product ion spectrum illustrated with Figure 3c. Dominating the BT CID spectrum are the charge-inverted 16:0 and 18:1 complex cations observed at *m/z* 459.2 and 485.2, respectively. As described previously, ion trap CID of $[FA − H + MgPhen]^+$ enables unambiguous FA identification. Exploiting reproducible mass spectral patterns, direct spectral interpretation or automated CID spectral matching to an established FA library can be utilized to pinpoint carbon-carbon double bond position(s) in unsaturated fatty acyl chains. In the case of $[18:1(9Z) – H + MgPhen]^+$ derived from the CL 16:0/18:1(9*Z*)/16:0/18:1(9*Z*) precursor ion, the C9=C10 double bond position was verified via appearance of the characteristic spectral gap indicative of double bond position (highlighted in green shading) in the resulting product ion spectrum and perturbation of the 14 Da product ion spacing, as the difference between *m/z* 345.2 and *m/z* 357.2 is 12 Da. We also note that the $[18:1(9Z) − H + MgPhen]^+$ CID spectrum can further be matched to the reference spectrum of oleic acid. In total, the results in Figure 3 clearly demonstrate that CLs can be identified exploiting a combination of negative ion mode CID and charge-inversion reactions on the resulting fatty acyl anions. Specifically, interrogation of the CL dianion enables the identification of FA and PA composition, while charge-inversion ion/ion chemistry details the site(s) of unsaturation in fatty acyl constituents, permitting unambiguous structural identification and isomeric discrimination. Ultimately, the overall approach described here provides the complementary structural information from both ion polarities using a single optimized set of ionization conditions.

Analysis of E. coli CL extract

The outlined approach was applied to the *de novo* characterization of unknown CLs in an *E. coli*. extract. The direct infusion negative ion mode nESI mass spectrum of an *E. coli*. CL extract is depicted in Figure 4a. The ion seen at *m/z* 693.5 was selected with unit mass resolution. Based on *m/z* measurement alone, the precursor ion observed at *m/z* 693.5 ion can be classified at the sum compositional level as $[CL\ 67:3 – 2H]^{2−}$. Conducted within the collision cell, CID of $[CL\ 67:3 – 2H]^{2−}$ supports identification of fatty acyl and PA composition (Figure 4b). The CID spectrum of the *m/z* 693.5 ion revealed the 16:1 (*m/z* 253.2), 16:0 (*m/z* 255.2), 17:1 (*m/z* 267.2), 18:1 (*m/z* 281.2), and 19:1 (*m/z* 295.2) fatty acyl carboxylate anions. From Figure 4b, the product ions at *m/z* 701.5, 741.5, 715.5, and 727.5 provide the sum composition of the PA moieties, corresponding to the PA 32:1, PA 35:2, PA 33:1, and PA 34:2 moieties, respectively. In turn, the presence of four individual PA product ions indicates the presence of at least two isomeric CL 67:3 structures. Together with the observed FA product anions, the dominant CL isomer is suggested to be composed of PA 16:0_17:1 and PA 16:1_18:1 units, while the PA 16:0_16:1 and PA 16:1_19:1 moieties

comprise the minor CL isomer. Moreover, product ions arising from loss of a single acyl chain confirm the proposed major and minor isomeric contributors. Specifically, the [CL 16:0_16:1_16:1_19:1 – H – 19:1]$^-$ product ion at *m/z* 1091.8 verifies the minor CL isomer assignment of CL (16:0_16:1)_(16:1_19:1). CID of [CL 67:3 – 2H]$^{2-}$ also promoted losses of the 16:1, 16:0, 17:1, and 18:1 fatty acids, giving rise to abundant product ions at *m/z* 1131.8, 1133.8, 1119.8, and 1105.8, respectively and confirming the major CL isomer assignment as CL (16:0_17:1)_(16:1_18:1).

To locate positions of unsaturation in fatty acyl substituents, we employed charge inversion ion/ion chemistry, as detailed above. Product anions generated via ion-trap CID were charge inverted via reaction with $[MgPhen_3]^{2+}$ reagent dications. Next, BT CID was utilized to generate [FA – H + MgPhen]$^+$ cations (Figure 4c). The BT CID spectrum reveals abundant product ions at *m/z* 457.2, 459.2, 471.2, 485.2, and 499.2, reflecting the charge-inverted 16:1, 16:0, 17:1, 18:1, and 19:1 complex cations, respectively. Mass-selection and CID of each unsaturated [FA – H + MgPhen]$^+$ cation permitted the location of carbon-carbon double bonds and cyclopropane motifs. In general, the 18:1 and 16:1 fatty acyl substituents contain carbon-carbon double bonds, whereas the odd chain 17:1 and 19:1 carboxylate product cations contain cyclopropane rings. The CID spectra of the charge-inverted 18:1 (*m/z* 485.2), 16:1 (*m/z* 457.2), 17:1 (*m/z* 471.2), and 19:1 (*m/z* 499.2) ions are presented in Figure 5. From Figure 5a, the 18:1 fatty acyl was identified as 18:1(11) based on *de novo* interpretation and comparison to the *cis*-vaccenic acid reference spectrum. Briefly, the *m/z* 359.1 and 415.1 product ions formed via C9–C10 and C13–C14 fragmentation flank the characteristic spectral gap (highlighted in green shading) indicative of the C11=C12 double bond position. Additionally, perturbation of the usual 14 Da spacing between product ions further confirms double bond localization, as the *m/z* difference between the product ions at *m/z* 373.1 and 385.1 is 12 Da. Furthermore, the data suggest the 18:1 fatty acyl chain is comprised of greater than 95% 18:1(11), as evidence for alternate 18:1 isomers was not observed.[42] Ion trap CID of the [16:1 – H + MgPhen]$^+$ (*m/z* 457.2) lead to the assignment of the 16:1 fatty acyl as FA 16:1(9). Again, comparison to the palmitoleic acid reference CID spectrum as well as the location of the spectral gap (Figure 5b) permits the localization of the C9=C10 double bond in the 16:1 acyl chain. The cyclopropane structures in the 17:1 and 19:1 fatty acyls are confirmed by CID of the [17:1 – H + MgPhen]$^+$ (*m/z* 471.2) (Figure 5c) and [19:1 – H + MgPhen]$^+$ (*m/z* 499.2) (Figure 5d) complex cations, respectively. Ultimately, the observed spectral patterns following interrogation of the charge-inverted 17:1 and 19:1 ions are inconsistent with the presence of carbon-carbon double bonds, and, importantly, are indicative of the presence of cyclopropane motifs. While comparison to reference spectrum derived from a phytomonic acid standard enables confident identification of the 19:1 fatty acyl as 19:1(c11), an authentic reference standard for the 17:1 cyclopropane FA is not commercially available. In turn, the assignment of the cyclopropane ring position in the [17:1 – H + MgPhen]$^+$ complex cation relies exclusively on direct spectral interpretation, exploiting the observed spectral pattern and characteristic neutral losses. The data show three fragment ions at *m/z* 373.1, 387.1, and 415.1, respectively, arising from the tell-tale neutral losses of 98, 84, and 56 Da thus locating the cyclopropane ring at *n*-7 (i.e., c9) on the 17:1 fatty acyl chain (Figure 5c). Neutral loss plots shown in Figure 6 confirm the cyclopropane FA assignments.

Taken together, the negative ion mode CID spectrum of $[CL\ 67:3 - 2H]^{2-}$ in combination with the information obtained from the charge inversion experiments, reveal the major isomeric contributor to CL 67:3 derived from *E. coli* to be CL (16:0_17:1(c9))_(16:1(9)_18:1(11)), which agrees with a previous report.[39] Notably, a minor isomeric CL 67:3 structure was also assigned as CL (16:0_16:1(9))_(16:1(9)_19:1(c11)). In turn, the presented strategy affords the unambiguous, high-level cardiolipin structural identification, including the location of carbon-carbon double bond and cyclopropane unsaturation sites in fatty acyl constituents. Moreover, the incorporation of ion/ion chemistry in combination with low-energy CID experiments conducted in both ion polarities enables isomer distinction, as at least two isomeric CL contributors, both major and minor, were effectively resolved utilizing the developed approach.

Conclusions

We demonstrated here a top-down shotgun lipidomics approach for the structural elucidation of CLs that employs gas-phase charge inversion ion/ion chemistry. Specifically, doubly deprotonated CLs were first generated via negative nESI. Next, CID of the isolated $[CL - 2H]^{2-}$ dianion liberated fatty acyl carboxylate anions attached to the CL precursor ion at the *sn*-1, *sn*-2, *sn*-1', and *sn*-2' positions. The resulting CID spectra provide partial CL characterization, as individual PA moieties linked at the 1′- or 3′-positions of the glycerol backbone and fatty acyl substituents can be assigned. Following the generation of the $[FA - H]^-$ product ions from the CL precursor anion, the carboxylate anions are converted to $[FA - H + MgPhen]^+$ cations via gas-phase ion/ion reaction with $[MgPhen_3]^{2+}$ dications. Importantly, $[FA - H + MgPhen]^+$ cations can be isolated and dissociated to yield product ion spectra that enable unambiguous isomeric discrimination, including the localization of carbon-carbon double bond position(s). Furthermore, the CID spectra of $[FA - H + MgPhen]^+$ also reveal the presence and position of cyclopropane rings, differentiating these structures from their isomeric mono-unsaturated FA counterparts. Interestingly, cyclopropane FAs in E. coli CL extract were assigned at the *n*-7 position (relative to the methyl end of the chain). These data confirm that the cyclopropane FA 17:1(c9) and FA 19:1(c11) are regiochemically related to the *n*-7 monounsaturated chains, FA 16:1(9) and FA 18:1(11). This relationship is consistent with formation of the cyclopropane FAs through direct modification of the double bond in the monounsaturated FAs.[51]

Taken together, charge inversion ion/ion chemistry offers a sensitive, rapid, and entirely gas-phase MS^n process for detailed structural elucidation of CL. Major advantages of this approach include (i) the decoupling of ionization and derivatization events, permitting lipid ionization and characterization to be conducted independently and, in some cases, in opposite polarity, and (ii) the ability to differentiate subtle structural features like unsaturation elements including cyclopropane modifications utilizing a single derivatization platform. As demonstrated with the analysis of *E. coli* CL extract, the use of ion/ion chemistry allows for the identification of major, and some minor, isomeric contributors that are unresolved using conventional ESI-MS/MS experiments.

Supplementary Material

Refer to Web version on PubMed Central for supplementary material.

Acknowledgments

The authors acknowledge David Marshall for his extensive help and valuable discussions regarding mechanistic possibilities. This work was supported by the National Institutes of Health (NIH) under Grants GM R37-45372 and GM R01-118484. S.J.B. acknowledges project funding through the Discovery Program (DP190101486) Australian Research Council (ARC).

References

1. Pulfer M; Murphy RC, Electrospray mass spectrometry of phospholipids. Mass Spectrom. Rev 2003, 22 (5), 332–364. [PubMed: 12949918]
2. Murphy RC Tandem Mass Spectrometry of Lipids: Molecular Analysis of Complex Lipids 2015, (4), 1–280.
3. Han XL; Gross RW, Shotgun lipidomics: Electrospray ionization mass spectrometric analysis and quantitation of cellular lipidomes directly from crude extracts of biological samples. Mass Spectrom.y Rev 2005, 24 (3), 367–412.
4. Han XL; Yang K; Yang JY; Cheng H; Gross RW, Shotgun lipidomics of cardiolipin molecular species in lipid extracts of biological samples. J. Lipid Res 2006, 47 (4), 864–879. [PubMed: 16449763]
5. Wang M; Wang CY; Han RH; Han XL, Novel advances in shotgun lipidomics for biology and medicine. Prog. Lipid Res 2016, 61, 83–108. [PubMed: 26703190]
6. Mitchell TW; Pham H; Thomas MC; Blanksby SJ, Identification of double bond position in lipids: From GC to OzID. J. Chromatogr. B: Anal. Technol. Biomed. Life Sci 2009, 877 (26), 2722–2735.
7. Blanksby SJ; Mitchell TW, Advances in Mass Spectrometry for Lipidomics. In Annual Rev. Anal. Chem, Vol 3, Yeung ES; Zare RN, Eds. 2010; Vol. 3, pp 433–465.
8. Hancock SE; Poad BLJ; Batarseh A; Abbott SK; Mitchell TW, Advances and unresolved challenges in the structural characterization of isomeric lipids. Anal. Biochem 2017, 524, 45–55. [PubMed: 27651163]
9. Schlame M, Thematic review series: Glycerolipids - Cardiolipin synthesis for the assembly of bacterial and mitochondrial membranes. J. Lipid Res 2008, 49 (8), 1607–1620. [PubMed: 18077827]
10. Houtkooper RH; Vaz FM, Cardiolipin, the heart of mitochondrial metabolism. Cell. Molec. Life Sci 2008, 65 (16), 2493–2506. [PubMed: 18425414]
11. Lewis R; McElhaney RN, The physicochemical properties of cardiolipin bilayers and cardiolipin-containing lipid membranes. Biochim. Biophys. Acta Biomembranes 2009, 1788 (10), 2069–2079.
12. Scherer M; Schmitz G, Metabolism, function and mass spectrometric analysis of bis(monoacylglycero)phosphate and cardiolipin. Chem. Phys. Lipids 2011, 164 (6), 556–562. [PubMed: 21704024]
13. Schlame M; Ren MD, Barth syndrome, a human disorder of cardiolipin metabolism. Febs Letters 2006, 580 (23), 5450–5455. [PubMed: 16973164]
14. Chicco AJ; Sparagna GC, Role of cardiolipin alterations in mitochondrial dysfunction and disease. Am. J. Physiol. Cell Physiol 2007, 292 (1), C33–C44. [PubMed: 16899548]
15. Han XL; Yang JY; Yang K; Zhao ZD; Abendschein DR; Gross RW, Alterations in myocardial cardiolipin content and composition occur at the very earliest stages of diabetes: A shotgun lipidomics study. Biochem. 2007, 46 (21), 6417–6428. [PubMed: 17487985]
16. Kiebish MA; Han XL; Cheng H; Chuang JH; Seyfried TN, Cardiolipin and electron transport chain abnormalities in mouse brain tumor mitochondria: lipidomic evidence supporting the Warburg theory of cancer. J. Lipid Res 2008, 49 (12), 2545–2556. [PubMed: 18703489]

17. Paradies G; Paradies V; Ruggiero FM; Petrosillo G, Cardiolipin and Mitochondrial Function in Health and Disease. Antioxidants Redox Signaling 2014, 20 (12), 1925–1953. [PubMed: 24094094]

18. Sapandowski A; Stope M; Evert K; Evert M; Zimmermann U; Peter D; Page I; Burchardt M; Schild L, Cardiolipin composition correlates with prostate cancer cell proliferation. Molec. Cell. Biochem 2015, 410 (1–2), 175–185. [PubMed: 26314254]

19. Dudek J; Hartmann M; Rehling P, The role of mitochondrial cardiolipin in heart function and its implication in cardiac disease. Biochimica Et Biophysica Acta-Molecular Basis of Disease 2019, 1865 (4), 810–821. [PubMed: 30837070]

20. Oemer G; Lackner K; Muigg K; Krumschnabel G; Watschinger K; Sailer S; Lindner H; Gnaiger E; Wortmann SB; Werner ER; Zschocke J; Keller MA, Molecular structural diversity of mitochondrial cardiolipins. Proc. Natl. Acad. Sci. U. S. A 2018, 115 (16), 4158–4163. [PubMed: 29618609]

21. Hsu FF; Turk J; Rhoades ER; Russell DG; Shi YX; Groisman EA, Structural characterization of cardiolipin by tandem quadrupole and multiple-stage quadrupole ion-trap mass spectrometry with electrospray ionization. J. Am. Soc. Mass Spectrom 2005, 16 (4), 491–504. [PubMed: 15792718]

22. Ekroos K; Ejsing CS; Bahr U; Karas M; Simons K; Shevchenko A, Charting molecular composition of phosphatidylcholines by fatty acid scanning and ion trap MS3 fragmentation. J. Lipid Res 2003, 44 (11), 2181–2192. [PubMed: 12923235]

23. Hsu FF; Turk J, Characterization of cardiolipin from Escherichia coli by electrospray ionization with multiple stage quadrupole ion-trap mass spectrometric analysis of M-2H+Na (−) ions. J. Am. Soc. Mass Spectrom 2006, 17 (3), 420–429. [PubMed: 16442306]

24. Hsu FF; Turk J, Characterization of cardiolipin as the sodiated ions by positive-ion electrospray ionization with multiple stage quadrupole ion-trap mass spectrometry. J. Am. Soc. Mass Spectrom 2006, 17 (8), 1146–1157. [PubMed: 16750386]

25. Randolph CE; Fabijanczuk KC; Blanksby SJ; McLuckey SA, Proton transfer reactions for the gas-phase separation, concentration, and identification of cardiolipins. Anal. Chem, 2020.

26. Ma XX; Xia Y, Pinpointing Double Bonds in Lipids by Paterno-Buchi Reactions and Mass Spectrometry. Angewandte Chemie Int. Ed 2014, 53 (10), 2592–2596.

27. Ma XX; Chong L; Tian R; Shi RY; Hu TY; Ouyang Z; Xia Y, Identification and quantitation of lipid C=C location isomers: A shotgun lipidomics approach enabled by photochemical reaction. Proc. Natl. Acad. Sci. U. S. A 2016, 113 (10), 2573–2578. [PubMed: 26903636]

28. Stinson CA; Xia Y, A method of coupling the Paterno-Buchi reaction with direct infusion ESI-MS/MS for locating the C=C bond in glycerophospholipids. Analyst 2016, 141 (12), 3696–3704. [PubMed: 26892746]

29. Zhang WP; Zhang DH; Chen QH; Wu JH; Ouyang Z; Xia Y, Online photochemical derivatization enables comprehensive mass spectrometric analysis of unsaturated phospholipid isomers. Nat. Commun 2019, 10. [PubMed: 30602777]

30. Thomas MC; Mitchell TW; Blanksby SJ, Ozonolysis of phospholipid double bonds during electrospray ionization: A new tool for structure determination. J. Am. Chem. Soc 2006, 128 (1), 58–59. [PubMed: 16390120]

31. Thomas MC; Mitchell TW; Harman DG; Deeley JM; Murphy RC; Blanksby SJ, Elucidation of double bond position in unsaturated lipids by ozone electrospray ionization mass spectrometry. Anal. Chem 2007, 79 (13), 5013–5022. [PubMed: 17547368]

32. Thomas MC; Mitchell TW; Harman DG; Deeley JM; Nealon JR; Blanksby SJ, Ozone-induced dissociation: Elucidation of double bond position within mass-selected lipid ions. Anal. Chem 2008, 80 (1), 303–311. [PubMed: 18062677]

33. Thomas MC; Mitchell TW; Blanksby SJ, Online Ozonolysis Methods for the Determination of Double Bond Position in Unsaturated Lipids. In Lipidomics: Vol 1: Methods and Protocols, Armstrong D, Ed. 2009; Vol. 579, pp 413–441.

34. Poad BLJ; Pham HT; Thomas MC; Nealon JR; Campbell JL; Mitchell TW; Blanksby SJ, Ozone-Induced Dissociation on a Modified Tandem Linear Ion-Trap: Observations of Different Reactivity for Isomeric Lipids. J. Am. Soc. Mass Spectrom 2010, 21 (12), 1989–1999. [PubMed: 20869881]

35. Brown SHJ; Mitchell TW; Blanksby SJ, Analysis of unsaturated lipids by ozone-induced dissociation. Biochim. Biophys. Mol. Cell Bio. Lipids 2011, 1811 (11), 807–817.
36. Pham HT; Maccarone AT; Thomas MC; Campbell JL; Mitchell TW; Blanksby SJ, Structural characterization of glycerophospholipids by combinations of ozone- and collision-induced dissociation mass spectrometry: the next step towards “top-down” lipidomics. Analyst 2014, 139 (1), 204–214. [PubMed: 24244938]
37. Marshall DL; Criscuolo A; Young RS; Poad BL; Zeller M; Reid GE; Mitchell TW; Blanksby SJ, Mapping Unsaturation in Human Plasma Lipids by Data-Independent Ozone-Induced Dissociation. J. Am. Soc. Mass Spectrom 2019, 1–10. [PubMed: 30430435]
38. Blevins MS; Klein DR; Brodbelt JS, Localization of Cyclopropane Modifications in Bacterial Lipids via 213 nm Ultraviolet Photodissociation Mass Spectrometry. Anal. Chem 2019, 91 (10), 6820–6828. [PubMed: 31026154]
39. Macias LA; Feider CL; Eberlin LS; Brodbelt JS, Hybrid 193 nm Ultraviolet Photodissociation Mass Spectrometry Localizes Cardiolipin Unsaturations. Anal. Chem 2019, 91 (19), 12509–12516. [PubMed: 31490676]
40. Randolph CE; Foreman DJ; Betancourt SK; Blanksby SJ; McLuckey SA, Gas-phase ion/ion reactions involving tris-phenanthroline alkaline earth metal complexes as charge inversion reagents for the identification of fatty acids. Anal. Chem 2018, 90 (21), 12861–12869. [PubMed: 30260210]
41. Franklin ET; Betancourt SK; Randolph CE; McLuckey SA; Xia Y, In-depth structural characterization of phospholipids by pairing solution photochemical reaction with charge inversion ion/ion chemistry. Anal. Bioanal. Chem 2019.
42. Randolph CE; Foreman DJ; Blanksby SJ; McLuckey SA, Generating Fatty Acid Profiles in the Gas Phase: Fatty Acid Identification and Relative Quantitation Using Ion/Ion Charge Inversion Chemistry. Anal.Chem 2019, 91 (14), 9032–9040. [PubMed: 31199126]
43. Randolph CE; Blanksby SJ; McLuckey SA, Toward Complete Structure Elucidation of Glycerophospholipids in the Gas Phase through Charge Inversion Ion/Ion Chemistry. Anal. Chem 2019.
44. Randolph CE; Shenault DM; Blanksby SJ; McLuckey SA, Structural Elucidation of Ether Glycerophospholipids Using Gas-Phase Ion/Ion Charge Inversion Chemistry. J. Am. Soc. Mass Spectrom 2020, 31 (5), 1093–1103. [PubMed: 32251588]
45. Randolph CE; Blanksby SJ; McLuckey SA, Charge-switch derivatization of fatty acid esters of hydroxy fatty acids via gas-phase ion/ion reactions. Anal. Chim. Acta, 2020.
46. Randolph CE; Foreman DJ; Betancourt SK; Blanksby SJ; McLuckey SA, Gas-Phase Ion/Ion Reactions Involving Tris-Phenanthroline Alkaline Earth Metal Complexes as Charge Inversion Reagents for the Identification of Fatty Acids. Anal. Chem 2018, 90 (21), 12861–12869. [PubMed: 30260210]
47. Yu X; Jin W; McLuckey SA; Londry FA; Hager JW, Mutual storage mode ion/ion reactions in a hybrid linear ion trap. J. Am. Soc. Mass Spectrom 2005, 16 (1), 71–81. [PubMed: 15653365]
48. Xia Y; Liang XR; McLuckey SA, Pulsed dual electrospray ionization for ion/ion reactions. J. Am. Soc. Mass Spectrom 2005, 16 (11), 1750–1756. [PubMed: 16182558]
49. Londry FA; Hager JW, Mass selective axial ion ejection from a linear quadrupole ion trap. J. Am. Soc. Mass Spectrom 2003, 14 (10), 1130–1147. [PubMed: 14530094]
50. Liebisch G; Vizcaino JA; Kofeler H; Trotzmuller M; Griffiths WJ; Schmitz G; Spener F; Wakelam MJO, Shorthand notation for lipid structures derived from mass spectrometry. J. Lipid Res 2013, 54 (6), 1523–1530. [PubMed: 23549332]
51. Grogan DW; Cronan JE, Cyclopropane ring formation in membrane lipids of bacteria. Microbiol. Molecul. Bio. Rev 1997, 61 (4), 429–&.

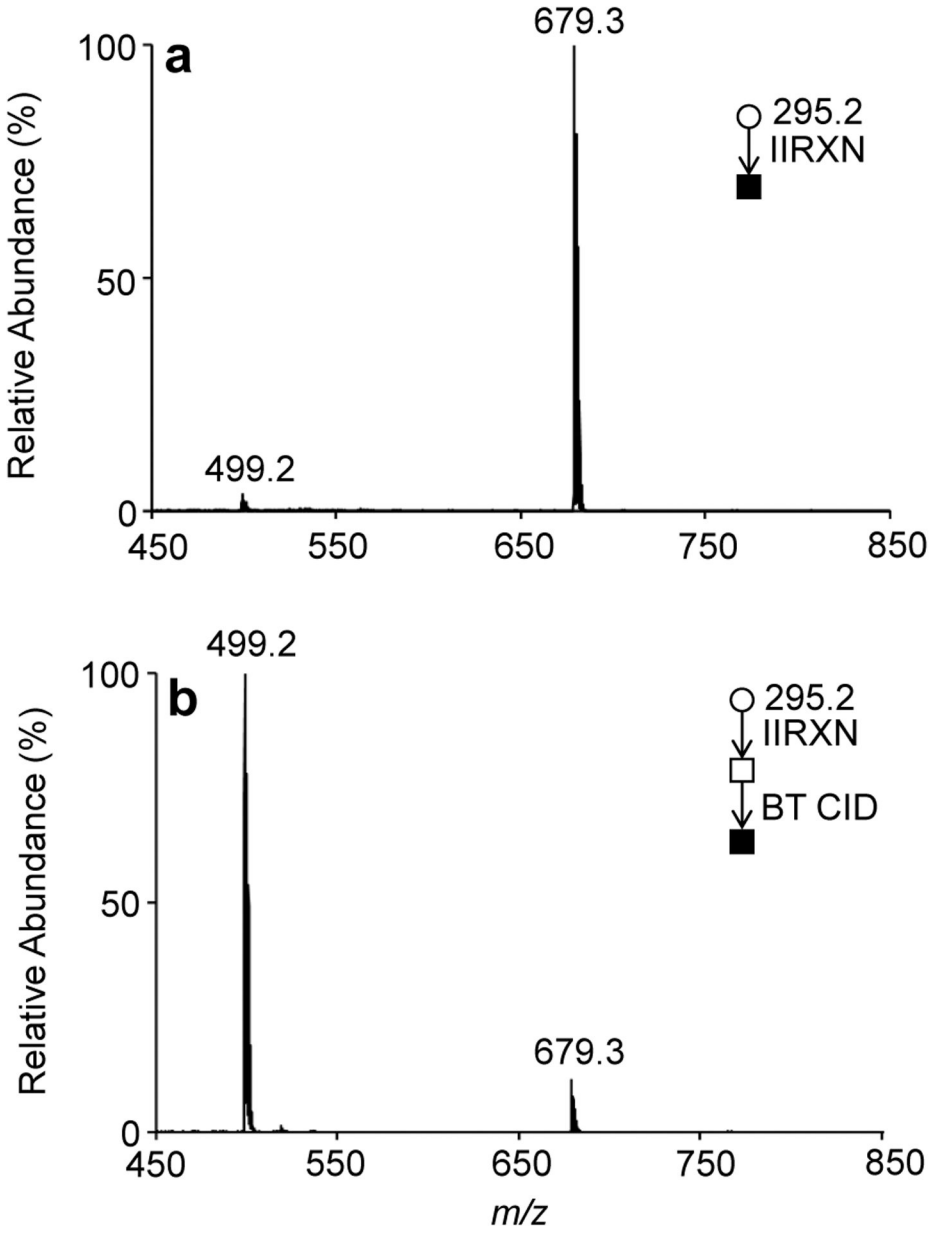

Figure 1.

Product ion spectra resulting from **(a)** the ion/ion reaction between $[19:1(c11) - H]^-$ anions and $[MgPhen_3]^{2+}$ dications and **(b)** ensuing BT collisional activation of the charge-inverted product ions shown in **(a)**.

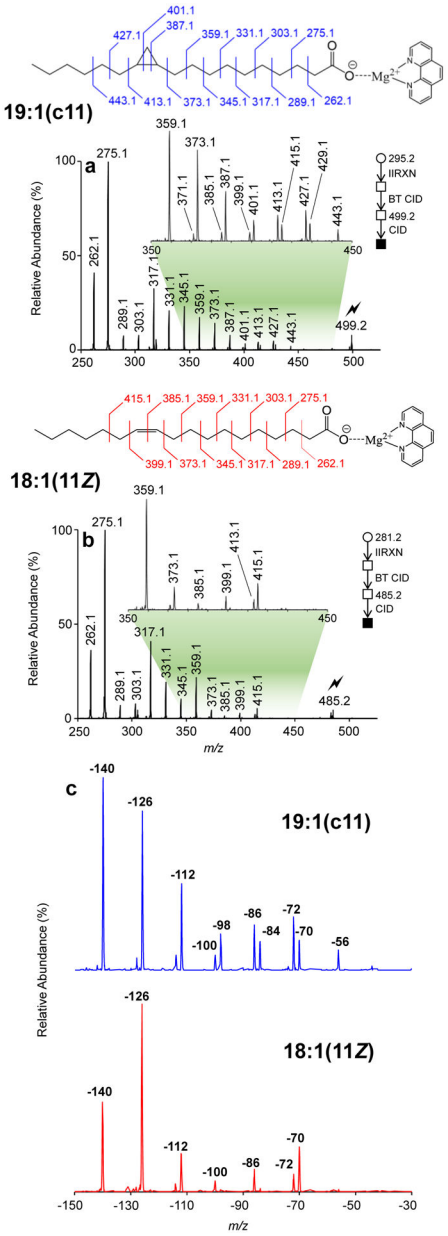

Figure 2.

Ion-trap CID spectra of **(a)** [19:1(c11) – H + MgPhen]$^+$ (*m/z* 499.2) and **(b)** [18:1(11*Z*) – H + MgPhen]$^+$ (*m/z* 485.2). (The product ion subjected to ion-trap CID is denoted with the lightning bolt (↯).) Neutral loss representations of the ion-trap CID spectra of **(c)** 19:1(c11) – H + MgPhen]$^+$ (*m/z* 499.2) and [18:1(11*Z*) – H + MgPhen]$^+$ (*m/z* 485.2) highlight the distinctive fragmentation patterns for the cyclopropane and double bonds, respectively.

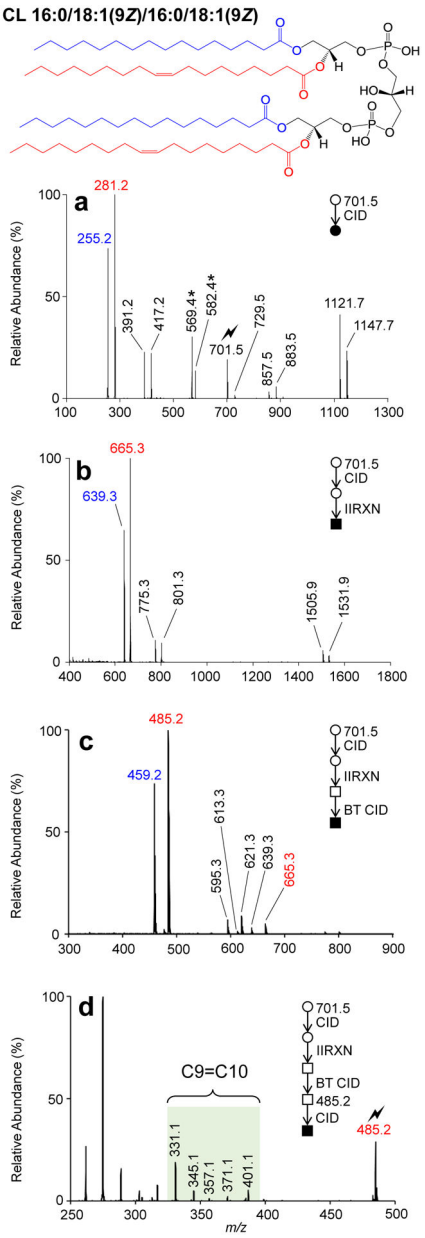

Figure 3.

Demonstration of charge inversion chemistry to elucidate CL structure. **(a)** Ion-trap CID spectrum of [CL 16:0/18:1(9*Z*)/16:0/18:1(9*Z*) – 2H]$^{2-}$ (*m/z* 701.5). Note that the asterisks (*) indicate doubly charged product ions. **(b)** Product ion spectrum resulting from the charge inversion of CL product ions shown in **(a)** upon ion/ion reaction with [MgPhen$_3$]$^{2+}$ reagent dications. **(c)** BT CID spectrum generated via activation of charge-inverted product ions shown in **(b)**. **(d)** Ion-trap CID spectrum of [18:1(9*Z*) – H + MgPhen]$^{+}$ (*m/z* 485.2).

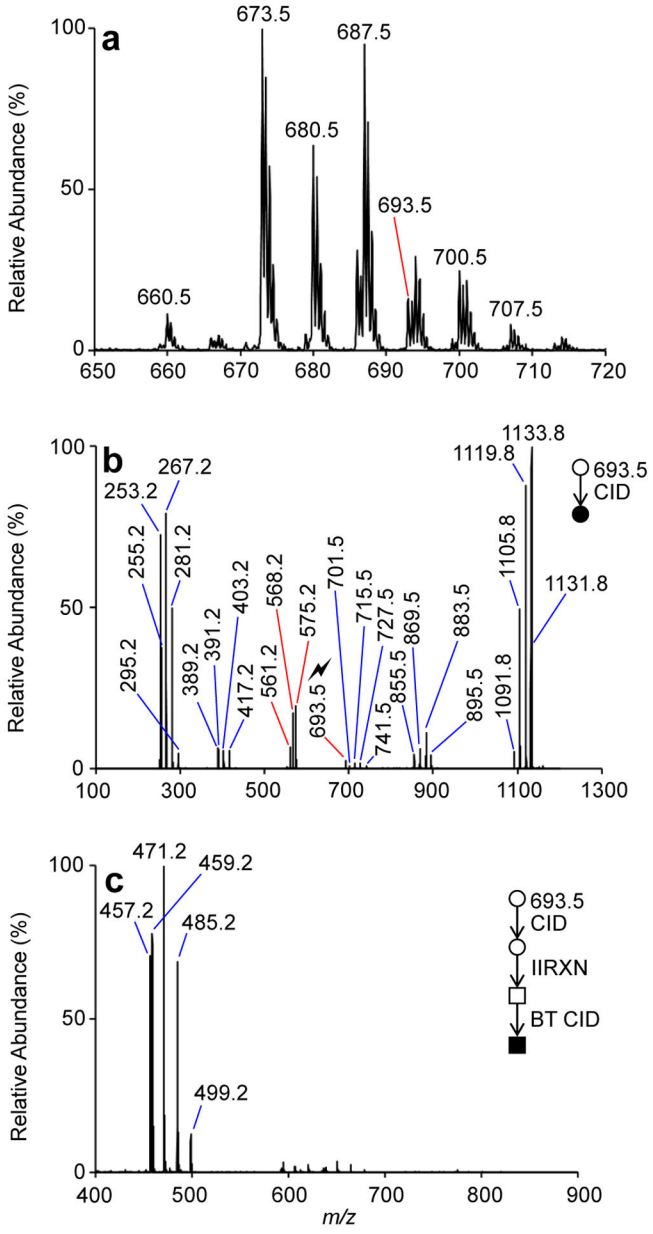

Figure 4.

(a) Direct infusion negative ion mode nESI mass spectrum of *E. coli*. CL extract. **(b)** Ion-trap CID spectrum of the mass-selected *m/z* 693.5 precursor anion derived from *E. coli*. CL extract. **(c)** Product ion spectrum resulting from the charge-inversion of product ions generated via CID of *m/z* 693.5 followed by activation via BT CID. Note that ions indicated with red lines are doubly charged, whereas those referenced with blue lines are singly charged.

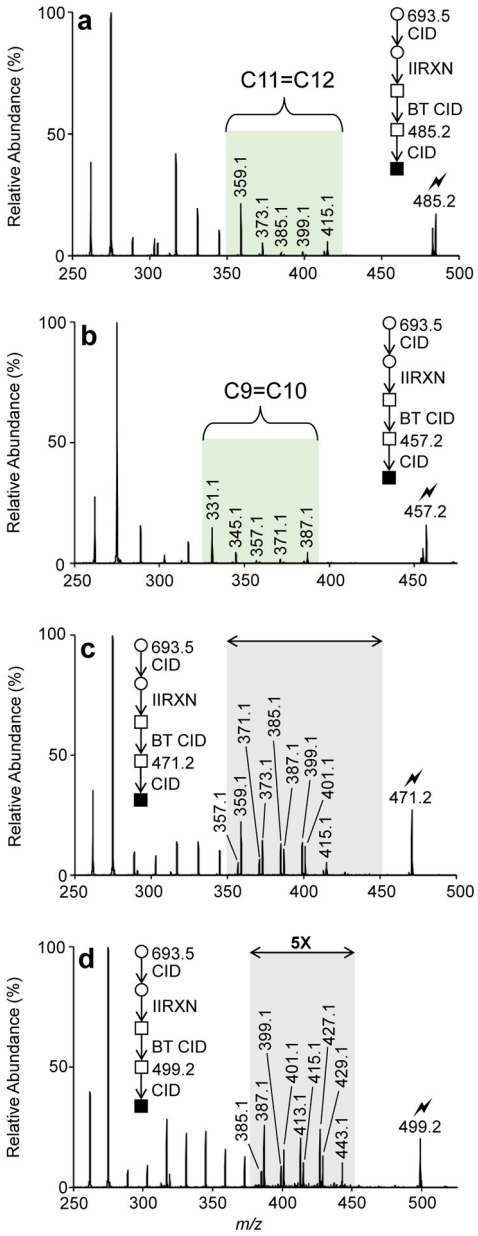

Figure 5.

Ion-trap CID spectra of the **(a)** [18:1 – H + MgPhen]$^+$ (*m/z* 485.2), **(b)** [16:1 – H + MgPhen]$^+$ (*m/z* 457.2), **(c)** [17:1 – H + MgPhen]$^+$ (*m/z* 471.2), and **(d)** [19:1 – H + MgPhen]$^+$ (*m/z* 499.2) obtained from CL 67:3 in *E. coli* extract.

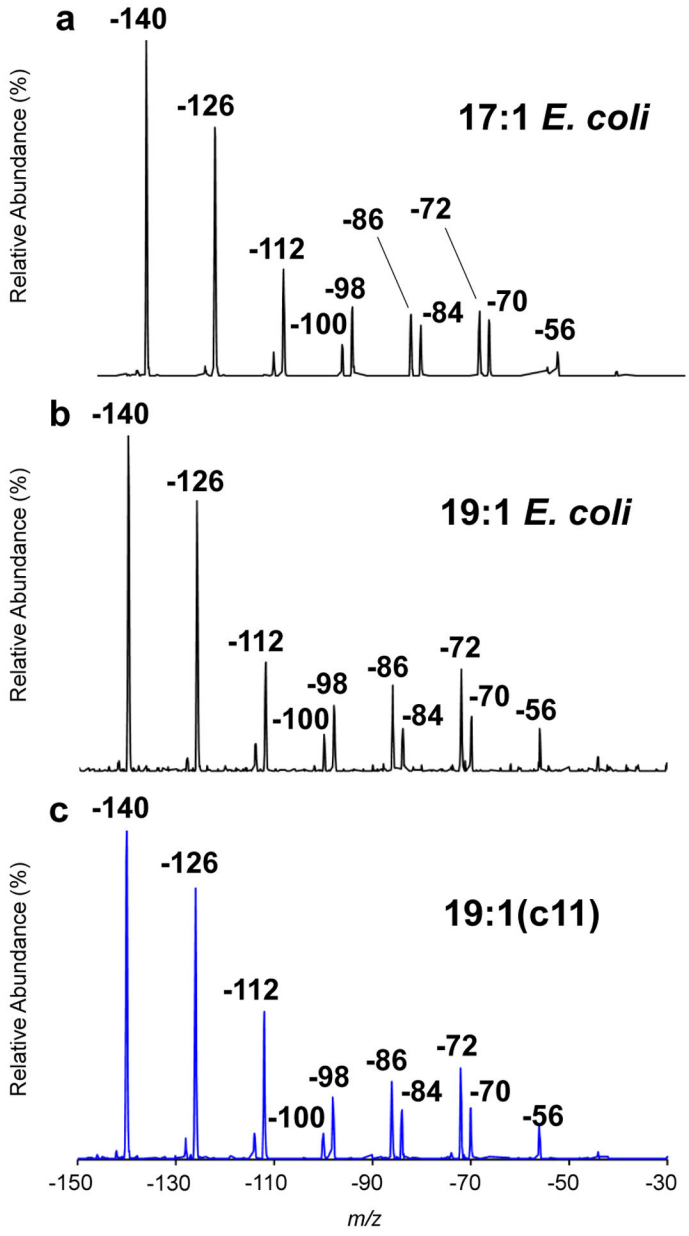

Figure 6.

Neutral loss representation of ion-trap CID spectra for **(a)** [17:1 – H + MgPhen]$^+$ (*m/z* 471.2), and **(b)** [19:1 – H + MgPhen]$^+$ (*m/z* 499.2) obtained from CL 67:3 in *E. coli* extract and (c) [19:1(c11) – H + MgPhen]$^+$ (*m/z* 499.2) obtained from an authentic reference standard.

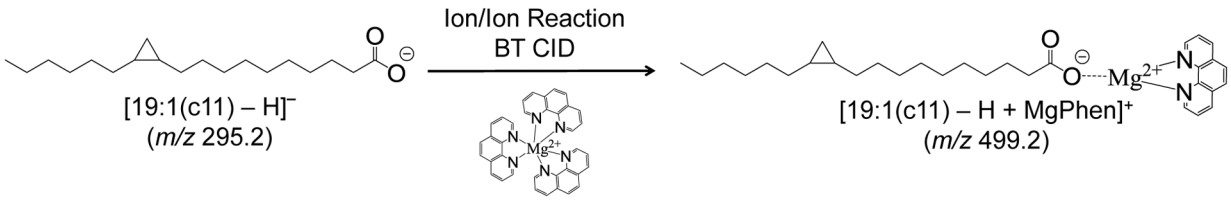

Scheme 1.

Singly deprotonated cyclopropane fatty acid ion reacts with $[MgPhen_3]^{2+}$ dications followed by beam-type CID to produce the $[FA - H + MgPhen]^+$ cation.

Table 1.

Predicted neutral losses for $[FA - H + MgPhen]^+$ product ions from cyclopropane FAs

Cyclopropyl Position	Predicted Neutral Loss (Da)
n-1	14
n-2	28
	14
n-3	42
	28
n-4	56
	42
	14
n-5	70
	56
	28
n-6	84
	70
	42
n-7	98
	84
	56
n-8	112
	98
	70
n-9	126
	112
	84
n-10	140
	126
	98
n-11	154
	140
	112
n-12	168
	154
	126